Double-mode RR Lyrae star — robust distance and metallicity indicators

Shu Wang[1,3], **Xiaodian Chen**[1,2,3], **Jianxing Zhang**[1,2] **and Licai Deng**[1,2,3]

[1]CAS Key Laboratory of Optical Astronomy, National Astronomical Observatories, Chinese Academy of Sciences, Beijing 100101, China
email: shuwang@nao.cas.cn

[2]School of Astronomy and Space Science, University of the Chinese Academy of Sciences, Beijing, 100049, China

[3]Department of Astronomy, China West Normal University, Nanchong, 637009, China

Abstract. RR Lyrae (RR Lyr) stars are a well-known and useful distance indicator for old stellar populations such as globular clusters and dwarf galaxies. Fundamental-mode RR Lyr (RRab) stars are commonly used to measure distances, and the accuracy of the determined distance is strongly constrained by metallicity. Here, we investigate the metallicity dependence in the period–luminosity (PL) relation of double-mode RR Lyr (RRd) stars. We find and establish a linear relation between metallicity and period or period ratio for RRd stars. This relation can predict the metallicity as accurately as the low-resolution spectra. Based on this relation, we establish a metallicity-independent PL relation for RRd stars. Combining the distance of the Large Magellanic Cloud and Gaia parallaxes, we calibrate the zero point of the derived PL relation to an error of 0.022 mag. Using RRd stars, we measure the distances of globular clusters and dwarf galaxies with an accuracy of 2-3% and 1-2%, respectively. In the future, RRd stars could anchor galaxy distances to an accuracy of 1.0% and become an independent distance ladder in the Local Group.

Keywords. RR Lyrae variable stars, RRd variable stars, distance indicators, metallicity, dwarf galaxies

1. Introduction

RR Lyrae (RR Lyr) stars are low-mass stars that have evolved to the horizontal branch stage and begin to pulsate as they move into the instability strip. The pulsation periods of RR Lyr stars are about 0.2 to 1.0 days. According to the pulsation mode, RR Lyr stars are classified into RRab (fundamental mode), RRc (first-overtone mode) and RRd (double or multiple mode) stars. In the Hertzsprung–Russell diagram, RRd stars are located in the intersection region of the instability strips of RRab and RRc stars.

Most RRd stars are clustered in a sequence on the Petersen diagram (Petersen 1973) and are called classical RRd stars. There are also anomalous and peculiar RRd stars. The anomalous or peculiar RRd stars are located above or below the sequence of classical RRd stars on the Petersen diagram (Nemec & Moskalik 2021). The dominant mode of the anomalous or peculiar RRd stars is the fundamental mode, while the dominant mode of classical RRd stars is the first-overtone mode. In addition, anomalous or peculiar RRd stars usually have long-term amplitude modulation. In this paper, the default RRd star is the classical RRd star.

RR Lyr stars were searched for by a large number of time domain survey, including the Optical Gravitational Lensing Experiment (OGLE, Soszyński et al. 2009; Soszynński et al. 2016, 2019), the Gaia (Clementini et al. 2022), the Zwicky Transient Facility (ZTF, Chen et al. 2020), the All-Sky Automated Survey for Supernovae (ASASSN, Jayasinghe et al. 2018), the Asteroid Terrestrial-impact Last Alert System (ATLAS, Heinze et al. 2018), the Wide-field Infrared Survey Explorer (WISE, Chen et al. 2018), and the PanSTARRS1(Sesar et al. 2017).

RR Lyr stars are good distance tracers for the old population. They satisfy the metallicity–luminosity (LZ) relation in the V band and the period–metallicity–luminosity (PLZ) relation in infrared bands. Since the two periods of RRd stars also satisfy the PLZ relation of RRab or RRc, respectively, RRd stars also have LZ and PLZ relations. Usually, RRd stars were not adopted to measure distances because the determined periods of RRd stars are not as accurate as those of RRab stars.

For RRd stars, both theory (Popielski et al. 2000; Marconi et al. 2015) and observations (Catelan & Smith 2015; Soszynński et al. 2019) suggest that compared to metal-poor RRd stars, metal-rich RRd stars have shorter fundamental periods and smaller period ratios. There seems to be a good linear relation between the period ratio and metallicity (Braga et al. 2022). In this work, we investigate the metallicity dependence in the period–luminosity (PL) relation of RRd stars and establish their PL relation (Chen et al. 2023).

2. Period–Metallicity Relation

We collect RRd stars mainly based on Gaia and OGLE databases. From Gaia DR3, we obtain 1021 Galactic RRd stars. From OGLE, we collect 2083 and 674 RRd stars belonging to the Large Magellanic Cloud (LMC) and the Small Magellanic Cloud (SMC), respectively. Metallicity information for these stars is taken from low-resolution spectra of the Sloan Digital Sky Survey (SDSS, Eisenstein et al. 2011) and the Large Sky Area Multi-Object Fiber Spectroscopic Telescope (LAMOST, Cui et al. 2012). After cross-matching, we obtain 100 RRd stars with SDSS or LAMOST metallicities. In addition, we supplement another 203 RRd stars with SDSS or LAMOST metallicity based on the ZTF data. The final sample contains 207 and 96 RRd stars with metallicity measurements from SDSS and LAMOST, respectively.

$$
\begin{aligned}
[\text{Fe/H}]_{\text{SDSS}} = & -(173 \pm 38)\left(\log \frac{P_{1\text{O}}}{P_{\text{F}}} - \log 0.745\right) \\
& -(6.62 \pm 0.88)(\log P_{1\text{O}} - \log 0.37) - (1.76 \pm 0.01), \\
[\text{Fe/H}]_{\text{LAMOST}} = & -(184 \pm 70)\left(\log \frac{P_{1\text{O}}}{P_{\text{F}}} - \log 0.745\right) \\
& -(5.69 \pm 1.50)(\log P_{1\text{O}} - \log 0.37) - (1.68 \pm 0.03),
\end{aligned}
\tag{1}
$$

Based on the selected RRd stars, we establish the period–period ratio–metallicity relation. The results are shown in equation 1. For the SDSS metallicity, the scatter σ is 0.16 dex and the correlation coefficient R^2 is 0.74. For the LAMOST metallicity, the scatter σ is 0.21 dex and the correlation coefficient R^2 is 0.60. The scatter of this relation decreases when a tighter criterion on metallicity error is adopted. For example, when we restrict the metallicity error to less than 0.04, with the rest of 56 RRd, the scatter of this relation will decrease to 0.13 dex. By comparing the scatter of the period–period ratio–metallicity relation with the external error of metallicity, we find that the metallicity estimated from the period and the period ratio of RRd stars can be as accurate as the low-resolution spectra.

With metallicities from high-resolution spectra, the scatter of the period–period ratio–metallicity relation could be greatly reduced. For example, for Cepheids, the scatter of
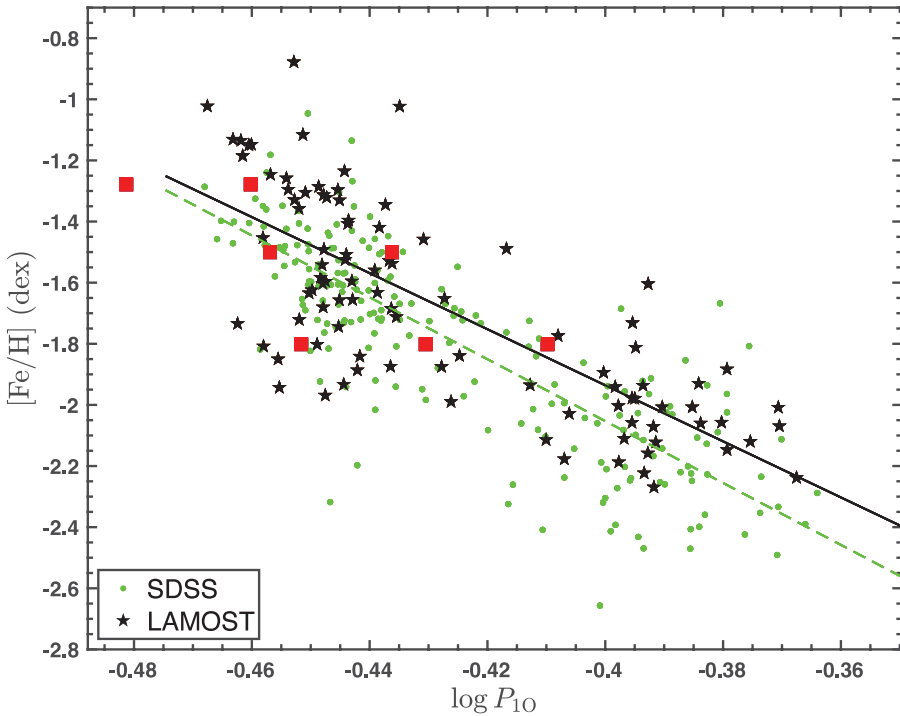
Figure 1. The Period–metallicity diagram of RRd stars with metallicities from SDSS (green dots) and LAMOST (black pentagrams). The green dashed line and the black solid line are linear fit lines. Red squares are the grid points of the theoretical model.

the relation is only 0.033 dex (Kovtyukh et al. 2016). In the future, with metallicities from high-resolution spectra, the period–period ratio–metallicity relation of RRd stars could also have a small scatter. Kovtyukh et al. (2016) found that for double–mode Cepheids, their metallicity depend on period ratio more than the period. Based on our sample, we find that RRd metallicity is more dependent on the period than the period ratio.

Figure 1 shows the distribution of RRd stars in the period–metallicity (PZ) diagram. The green dots and black pentagrams are RRd stars with metallicities from SDSS and LAMOST, respectively. Red squares are the grid points of the theoretical model (Marconi et al. 2015). There is an intuitive linear relationship between the metallicity and the period. The green dashed line and the black solid line are linear fit lines. The determined PZ relations for RRd stars with SDSS metallicities are listed in equation 2.

$$
\text{[Fe/H]}_{\text{SDSS}} = (-10.33 \pm 0.47)\log P_{\text{F}} + (-4.87 \pm 0.14), \sigma = 0.17\,\text{dex}, R^2 = 0.71,
$$
$$
\text{[Fe/H]}_{\text{SDSS}} = (-10.15 \pm 0.46)\log P_{\text{1O}} + (-6.11 \pm 0.19), \sigma = 0.17\,\text{dex}, R^2 = 0.71 \tag{2}
$$

3. Period–Luminosity Relation

Combining the PLZ relation with the period–period ratio–metallicity relation, the period–period ratio–luminosity relation is derived. We determined the period–period ratio–luminosity relation based on OGLE LMC RRd stars. We find that there is an approximate linear relation between the period and the period ratio, with a correlation coefficient of 0.7 and a dispersion of 0.0003. Therefore, we try to simplify the period–period ratio–luminosity relation to the period–luminosity (PL) relation. We find that the absolute magnitude difference predicted by the PL relation and the period–period ratio–luminosity relation is small. The scatter in magnitude difference is 0.01 mag and
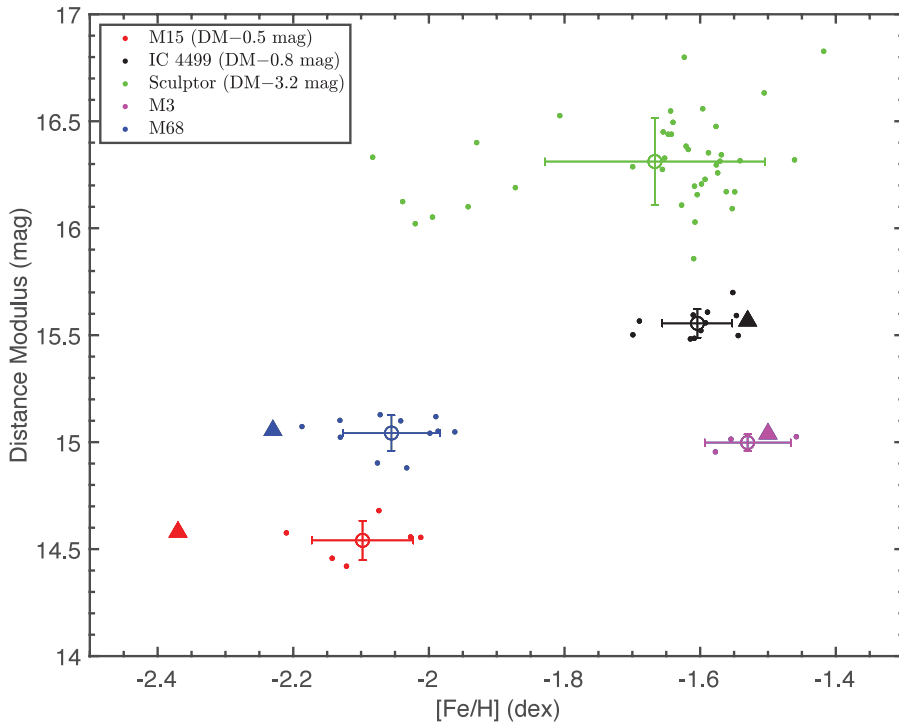
Figure 2. Metallicity and distance modulus (DM) determinations based on RRd stars for M15 (red dots), IC 4499 (black dots), Sculptor (green dots), M3 (magenta dots), and M68 (blue dots). The mean values of RRd stars in five targets are shown as open circles with 1σ internal errors. Solid triangles indicate the parameters of the four globular clusters from the Harris's globular cluster catalog. To make the figure clearer, the distance modulus of M15, IC 4499, and Sculptor are reduced by 0.5 mag, 0.8 mag, and 3.2 mag, respectively.

the maximum magnitude difference is only 0.06 mag. In addition, the scatter of the PL relation and the period–period ratio–luminosity relation is the same. Since the metallicity is more dependent on period, we ultimately simplify the period–period ratio–luminosity relation to the PL relation (see equation 3). Here, we adopt the Wesenheit magnitude (Madore 1982) i.e. $W_{VI} = I - 1.55(V - I)$ and $W_{G,BP,RP} = G - 1.90(BP - RP)$.

$$M_{W_{VI}} = (-4.523 \pm 0.156) \log P_{\mathrm{F}} + (16.620 \pm 0.048) - \mathrm{DM_{LMC}}, \sigma = 0.132 \,\mathrm{mag},$$
$$M_{W_{VI}} = (-4.434 \pm 0.153) \log P_{1\mathrm{O}} + (16.079 \pm 0.067) - \mathrm{DM_{LMC}}, \sigma = 0.132 \,\mathrm{mag},$$
$$M_{W_{G,BP,RP}} = (-3.623 \pm 0.229) \log P_{\mathrm{F}} + (17.042 \pm 0.071) - \mathrm{DM_{LMC}}, \sigma = 0.159 \,\mathrm{mag},$$
$$M_{W_{G,BP,RP}} = (-3.557 \pm 0.225) \log P_{1\mathrm{O}} + (16.606 \pm 0.098) - \mathrm{DM_{LMC}}, \sigma = 0.159 \,\mathrm{mag}$$
$$(3)$$

We combine the LMC distance (Pietrzyński et al. 2019) and Gaia parallaxes to calibrate the zero points of the PL relations as $M_{W_{G,BP,RP}}(P_{1\mathrm{O}} = 0.37\mathrm{d}) = -0.348 \pm 0.022$ mag and $M_{W_{VI}}(P_{1\mathrm{O}} = 0.37\mathrm{d}) = -0.496 \pm 0.022$ mag. Meanwhile, we derive the zero point of the Gaia DR3 parallax, which is 13.4 ± 5.8 μas. This parallax zero point agrees well with that determined by classical Cepheids (Riess et al. 2021).

4. Distance and Metallicity Measurements

The established PL relation and PZ relation of RRd stars can be used to determine the distances and metallicities of distant objects. We measure the distances and metallicities of four globular clusters (IC 4499, M15, M3, and M68) and a dwarf galaxy (Sculptor)

based on RRd stars with Gaia data. Figure 2 shows the derived metallicities and distance moduli. The different colored dots indicate individual metallicity and distance modulus determinations based on RRd stars in M15 (red), IC 4499 (black), Sculptor (green), M3 (magenta), and M68 (blue). Solid triangles indicate the results for the four globular clusters from the globular cluster catalog of Harris (1996). The mean values of RRd stars in five targets are shown as open circles with 1σ internal errors. For dwarf galaxy Sculptor, the distance accuracy is about 1.8%, and the metallicity dispersion is 0.2 dex. For globular clusters, the distance accuracy is about 2-3%, and the metallicity dispersion is 0.05 dex. Recently, we use RRd stars to measure the distances and metallicities of other dwarf galaxies. For example, we measure the distances and metallicities of five dwarf galaxies in M31, where the distance accuracy is about 1.8%. We also determine the distance of the Fornax dwarf galaxy with an accuracy of 1.2% based on ~ 130 RRd stars.

There are several advantages of adopting RRd stars as distance indicators. Since the RRd star PL relation is not affected by metallicity, the galaxy distance error can be optimized to 1.2% based on ~ 100 RRd stars. This accuracy is as good as the distance accuracy of the LMC. RRd stars are not rare, and they account for 3-5% of RR Lyr stars. The number of RRd stars in the SMC, LMC, and the Galactic halo is comparable to the total number of classical Cepheids in these galaxies. Moreover, distance measurements based on RRd stars are less affected by extinction and binarity than the classical Cepheids. RRd stars are the best distance indicators for dwarf galaxies. They can also provide metallicity information for distance measurements of RRab stars. In the future, the China Space Station Telescope and the Vera C. Rubin Observatory Legacy Survey of Space and Time will discover more RRd stars. The RRd star can be an independent distance ladder in the Local Group, used to check the Cepheid (Riess et al. 2022) and the tip of the red giant branch (Freedman et al. 2019) distance ladders.

5. Summary

We discover a period–(period ratio)–metallicity relation for RRd stars and find it can predict metallicity as accurately as the low-resolution spectra. We propose that the PL relation of RRd stars is not affected by the metallicity and derive the PL relation of RRd stars. The zero point of the PL relation is determined with an error of 0.022 mag (1.0% error in the distance). We find that RRd stars can anchor galaxy distances with an accuracy of 1-2% (dwarf galaxies) and 2-3% (globular clusters). In the Future, RRd stars will be established as an independent distance ladder in the Local Group.

Acknowledgements

References

Braga, V. F., Fiorentino, G., Bono, G., et al. 2022, *Monthly Notices of the Royal Astronomical Society*, 517, 5368

Catelan, M., & Smith, H. A. 2015, Pulsating Stars. (Wiley-VCH)

Chen, X., Wang, S., Deng, L., et al. 2018, *ApJS*, 237, 28

Chen, X., Wang, S., Deng, L., et al. 2020, *ApJS*, 249, 18

Chen, X., Zhang, J., Wang, S., & Deng, L. 2023, *Nat. Astron.*, arXiv:2306.10708

Clementini, G., et al., et al. 2022, *arXiv*, 2206.06278

Cui, X.-Q., et al. 2012, *Res. Astron. Astrophys.*, 12, 1197

Eisenstein, D. J., et al. 2011, *Astron. J.*, 142, 72

Freedman, W. L., et al. 2019, *ApJ*, 882, 34

Harris, W. 1996, *ApJ*, 112, 1487

Heinze, A. N. Tonry J. L., Denneau L., et al. 2018, *ApJ*, 156, 241

Jayasinghe, T., et al. 2018, *Monthly Notices of the Royal Astronomical Society*, 477, 3145

Kovtyukh, V., et al. 2016, *Monthly Notices of the Royal Astronomical Society*, 460, 2077

Madore, B. F. 1982, *ApJ*, 253, 575

Marconi, M., et al. 2015, *ApJ*, 808, 50

Nemec, J. M., & Moskalik, P. 2021, *MNRAS*, 507, 781

Petersen J. O. 1973, *A&A*, 27, 89

Pietrzyński, G., et al. 2019, *Nature*, 567, 200

Popielski, B. L., Dziembowski, W. A., Cassisi, S. 2000, *Acta Astron.*, 50, 491

Riess, A. G., et al. 2021, *ApJL*, 908, L6

Riess, A. G., et al. 2022, *ApJL*, 934, L7

Sesar, B. et al. 2017, *ApJ*, 153, 204

Soszyński, I. et al. 2009, *Acta Astron.*, 59, 1

Soszyński, I., et al. 2016, *Acta Astron.*, 66, 131

Soszyński, I., et al. 2019, *Acta Astron.*, 69, 321